Paris
France

The Potential of High Resolution Satellite Interferometry for Monitoring Enhanced Oil Recovery

Urs Wegmüller [a]
Lutz Petrat [b]
Karsten Zimmermann [c]
Issa al Quseimi [d]

1 Introduction

Over the last years land surface deformation monitoring using space-borne SAR interferometry became operational. Sensors used include mainly the C-band (ERS-1, ERS-2, ENVISAT, Radarsat-1) and L-band SAR Systems (JERS-1 and ALOS). Over the last year a new generation of SAR satellites (e.g. TerraSAR-X, Radarsat-2) was launched and interferometric data series are now operationally available. These new SAR sensors are characterized by high resolution modes. Furthermore, repeat-intervals shorter than the typical 35-day interval known from the widely used European C-band SAR systems are available.

High temporal and spatial resolution of these new SAR sensors reveal the potential of monitoring small-scale and highly dynamic surface movements, which are expected to be useful for monitoring more dynamic ground movements as occurring for example in the context of improved oil recovery methods.

To evaluate this potential we used high resolution TerraSAR-X SAR data for monitoring surface displacements over an oil field in the Middle East. To additionally support the quality of TerraSAR-X results a comparison with high precise DGPS measurements was performed. This contribution describes the processing done and summarizes the study results.

2 Objective

The objective of the study was to discuss data processing issues and results related to the differential interferometric processing of high resolution TerraSAR-X SAR data acquired over an oil field in the Middle East.

3 Input Data

3.1 TerraSAR-X Data

The TerraSAR-X satellite, launched in June 2007, is an X-Band SAR operating in different imaging modes. For our experiment a series of StripMap data sets was acquired over an oilfield in The Middle East. TerraSAR-X data were programmed and ordered by Infoterra Germany. The TerraSAR-X repetition cycle of 11-days was exploited as much as possible, yielding a data stack of 16 StripMap acquisitions between January and August 2008 (see Figure 1).

[a] GAMMA Remote Sensing AG, Switzerland, Email: wegmuller@gamma-rs.ch
[b] Infoterra GmbH, Germany, Email: lutz.petrat@infoterra-global.com
[c] DMT GmbH & Co. KG, Germany, Email: karsten.zimmermann@dmt.de
[d] Petroleum Development of Oman, Oman, Email: Issa.SS.Quseimi@pdo.co.om

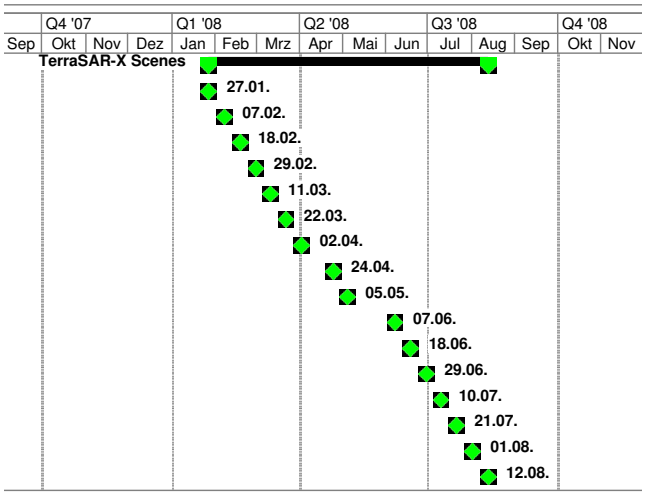


Figure 1: Acquisition Dates of available TerraSAR-X data

3.2 DGPS Data

GPS data were acquired by the oilfield operator at 74 locations in the oil field area. 69 of these points were measured campaign wise as rover stations at the time periods illustrated in Figure 2.

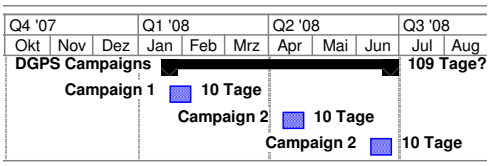


Figure 2: GPS campaigns in The Middle East oilfield

In total, 5 DGPS points (BAS1, REM1, REM2, REM3, REM4) were observed permanently, providing a daily set of coordinates.

4 Data Processing

4.1 Differential Radarinterferometry

4.1.1 SLC Data, Multi-looking, Geocoding

Single Look Complex (SLC) TerraSAR-X data were obtained (so called TerraSAR-X Single-look Slant-range Complex (SSC) data product). For the interferometric processing the GAMMA software was used.

Averaged multi-look intensity images of the full scene and the section chosen for the deformation monitoring are shown in Figure 3.

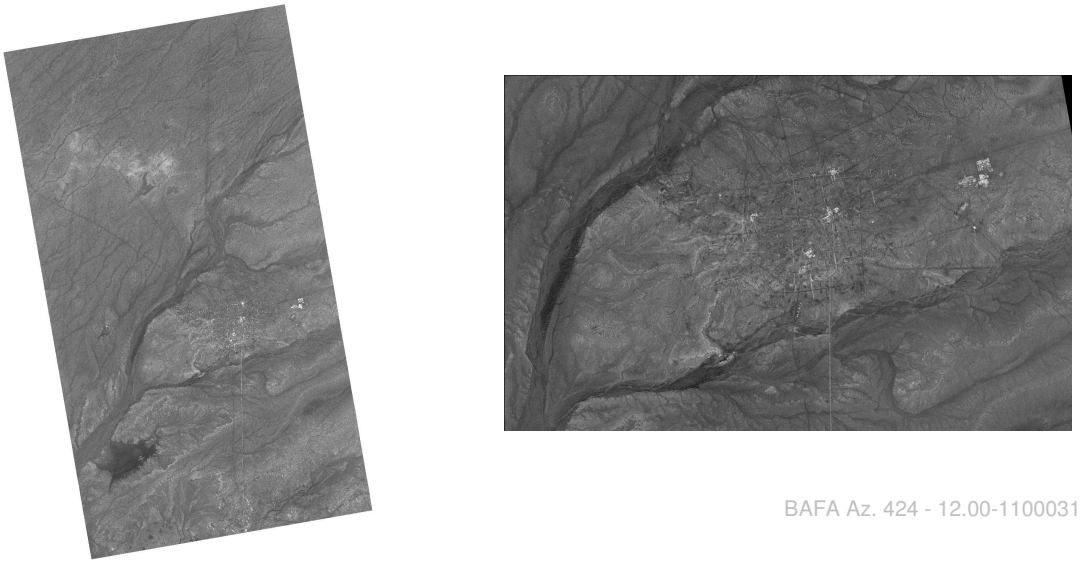


Figure 3: Multi-Look Intensity Image of (a) Full TerraSAR-X StripMap scene; (b) Area of Interest

Geocoding was performed on the multi-look intensity image for the area of interest. No special treatment was necessary and the state vectors looked accurate. As geometric reference representing the map geometry in the lookup table refinement a geocoded Landsat PAN image was used. The offsets which are corrected in the refinement step were only about 15 m in azimuth direction and about 8 m in slant-range (12 m in ground-range). The standard deviation of the individual offset estimates used in the refinement was below 2.5 m.

4.1.2 SLC Co-Registration

For SLC Co-registration, an approach was used, which considers local topography. This is expected to be relevant at this very high spatial resolution. The heights used in our case were SRTM heights which were transformed into the SAR multi-look geometry using the refined geocoding lookup table. This co-registration approach includes also a refinement step using actual offset estimates between the data sets and it provides error statistics. The SLC section on 5-May-2008 was used as reference geometry. Offsets determined in a test for the co-registered SLC's showed a very low standard deviation below 0.05 SLC pixels.

4.1.3 Differential Interferogram Generation

Initially, differential interferograms for all combinations and the entire area were generated. This was done for several reasons:

- Estimation of orbital phase trends,
- derivation of dependence of coherence on ground cover, baseline and time interval,
- collection of experience regarding level, spatial scale, and location of deformation, atmospheric effects, and other phase effects (e.g. caused by incorrect DEM),
- data quality checking.

Examples of a differential interferogram and of an RGB composite of coherence (red), backscatter (green) and backscatter ratio (blue) are shown in Figure 4 for a 11-day pair in summer (Figure 4 (a), (b), respectively.

The specific differential interferometric phase shown includes:

- 1-2 phase cycles of residual orbital phase
- atmospheric phase (of the order of 1 phase cycle)
- deformation phase
- residual topographic phase

Deformation phase is only clearly visible locally in areas where it dominates over the typical level of atmospheric phase.

The X-band coherence is high for most of the area over the 11-day periods considered. Over longer periods the coherence gets reduced and in local areas with high deformation rates it gets difficult to correctly resolve the interferometric phase.

Because of these observations, it was decided to use differential interferograms for a series of consecutive intervals for the further analysis, i.e. A-B, B-C, C-D, etc. For the late winter pairs these 11 or 22-day differential interferograms could be efficiently unwrapped after an initial strong multi-looking. This approach is well suited to estimate the spatially lower resolution component of the differential interferometric phase. This lower resolution component corresponds mainly to atmospheric phase, but it can, of course, also include deformation. For TerraSAR-X the spatial resolution is high, so that the typical deformation cones are included in this low-resolution component. This approach worked well for most of the area. The exception were small but very important areas with strong deformation and very high phase gradients (= high deformation gradients). For these local areas spatial unwrapping was done at the full resolution of the data without prior multi-looking of the interferograms. Furthermore, the solutions were manually checked and in a few cases corrected for obvious ambiguity errors.

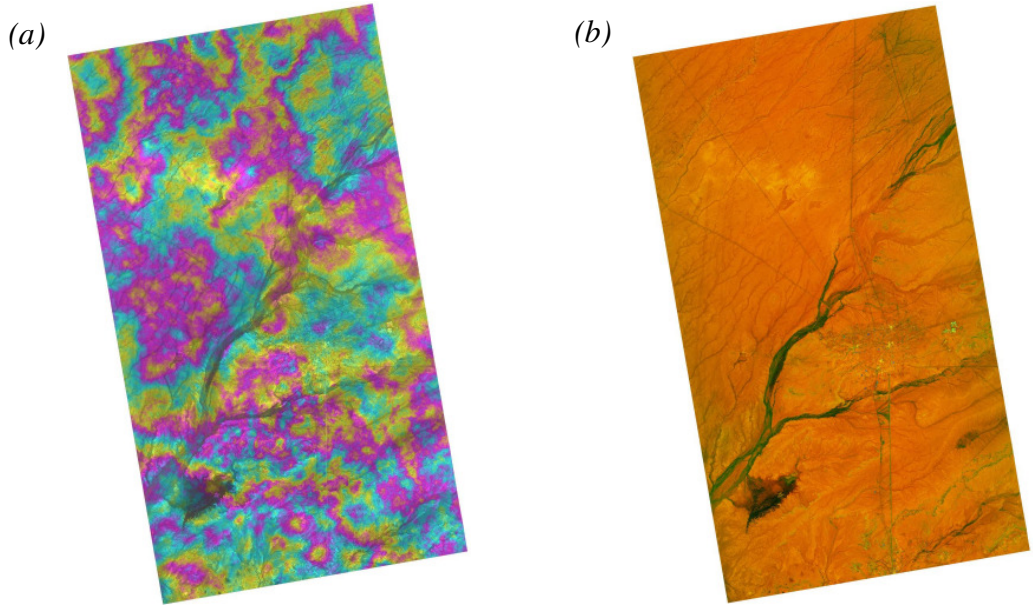


Figure 4: (a) Differential Interferogram derived from TerraSAR-X acquisitions 21/07/2008 and 01/08/2008; (b) RGB of coherence σ°, σ°-ratio related to (c)

For the sub-section this processing was applied for a chain of subsequent pairs (A-B, B-C, C-D, …) of 11 days temporal baselines. For each of these pairs orbital phase was unwrapped and orbital phase was subtracted. In order not to subtract deformation at low spatial scale no atmospheric phases were subtracted. The unwrapped phases relative to a selected reference point were then converted to vertical displacements (LOS component converted to total displacement under assumption that movement is in vertical direction).

4.2 DGPS

Precise GPS measurements and a state of the art post processing analysis enable to determine high accuracy point coordinates. Results can be mathematically evaluated regarding their quality, i.e. their internal and external accuracy.

The accuracy of GPS point measurement depends among other things on the accuracy of the satellite orbit and atmospheric interferences of signal transmission. Latest available software incorporates these factors very well due to precise orbit data, latest atmospheric models and noise eliminating techniques during data processing.

Figure 5 gives an example for the high external accuracy and shows the coordinate differences of daily solutions of station REM 1 in relation to the fixed reference station BAS 1. The daily solutions have horizontal coordinate differences lower then 1 mm and height difference lower then 2 mm. Joining all daily solutions to a weekly solution leads to accuracies of sub-millimeter level.

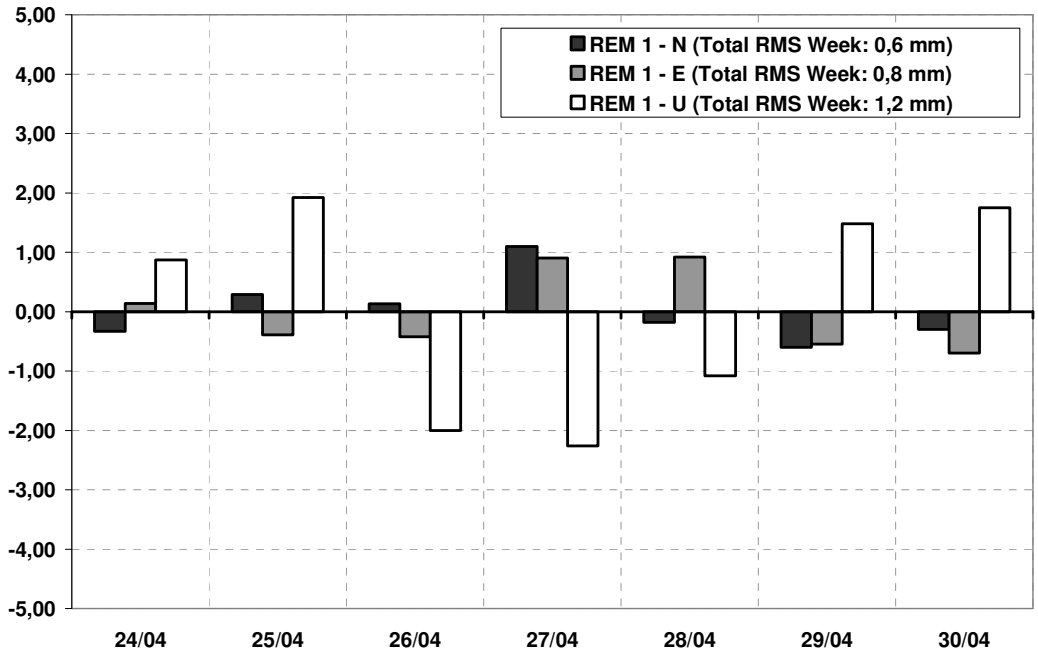


Figure 5: Repeatability of daily solutions of GPS station REM 1 (ordinate in mm)

All GPS rover points were analyzed campaign wise in order to enable a large scale comparison of results with the corresponding TerraSAR-X deformation map. During the acquisition period of TerraSAR-X the reference station (BAS1) and four locations (REM1, REM2, REM3, REM4) were processed in more detail and provided with a daily sampling of coordinates to also enable monitoring of dynamic ground movements.

5 Results

5.1 Monitoring of large scale subsidence pattern

In the short interval pairs the atmospheric distortions are severe. Only strong local deformation can reliably be identified and quantified. There remains an atmosphere related error of the order of 1 cm.

In the integrated solution the relative importance of the atmospheric path delay heterogeneity is reduced because more deformation (and consequently deformation phase) occurs over longer periods. The large scale subsidence in the center of the area shown becomes clearly visible. About 5 cm of subsidence is observed in this area which dominates clearly over the typical 1 cm atmospheric error (Figure 6).

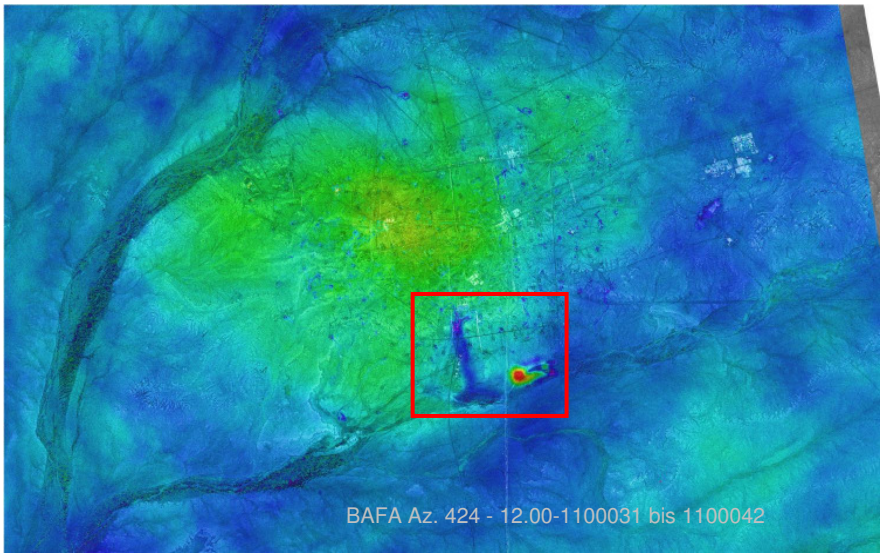


Figure 6: TerraSAR-X derived large scale and uniform surface movements and area of interest of highly dynamic surface movements (red rectangle)

The temporal evolution of the large scale surface displacements is shown in Figure 7.

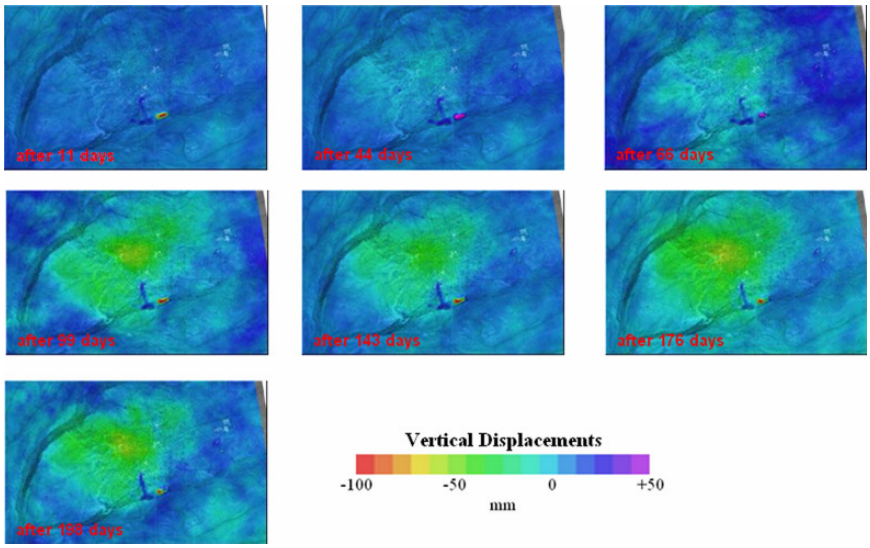


Figure 7: Evolution of TerraSAR-X derived large scale vertical displacements

5.2 Localized, Highly Dynamic Surface Movements

Apart from the large scale surface movement above the oilfields we observed localized areas of specific surface movement phenomena. Highly dynamic surface movements were identified in a sub-set area marked with a red rectangle in Figure 6.

The illustration of the temporal evolution of surface displacements shown in Figure 7 demonstrates the high dynamic of the surface movement in this area. Two signals can be identified in each surface displacement map of this figure, which can be separated due to their different temporal behavior:

First, a strong uplift signal in the west can be identified in the beginning of the observation period. Uplift decreases after a duration of approx. 22 days. This initial uplift detected by TerraSAR-X can be well approved by GPS measurements. Permanently measured GPS point "REM 1" is located near to the uplift zone. Figure 11 shows the location and almost identical vertical movement detected by both GPS and TerraSAR-X.

Second, a signal which is very rapidly changing from subsidence to uplift can be observed in the eastern part of the chosen sub-set in Figure 7. It has an extent of about 1200 m in length and approx. 400 m in width. This signal changes during the observed period from subsidence to uplift then again to subsidence and again to uplift with temporally varying but high movement rates. Displacement maps derived from the last 11 days interferogram indicate that the signal decayed to an uplift of lower amplitude.

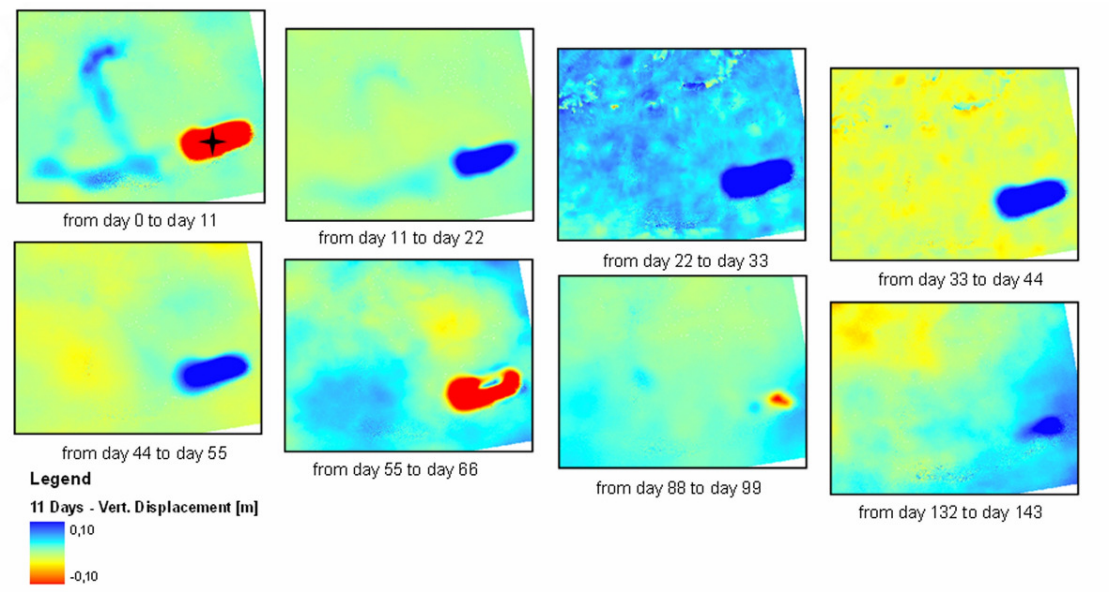


Figure 8: Oilfield related anomaly and sample evolution of TerraSAR-X – 11 days vertical displacements

The consecutive short-term vertical displacements extracted for one specific point (see black cross in Figure 8, first displacement map in time series), illustrate the temporal evolution of the movement (see Figure 9). Daily vertical displacements were calculated by dividing the displacement value at the chosen point by the temporal baseline (in days) of the related interferogram.

These daily vertical displacements were then related to the intermediate between the two SAR acquisition dates used for interferogram calculation. This approach allows estimating the temporal behavior of the signal.

The dynamic character of the signal with uplift and subsidence at rates up to approx. 10 mm/day is clearly visible. Unfortunately, there was no GPS point in this area for comparison.

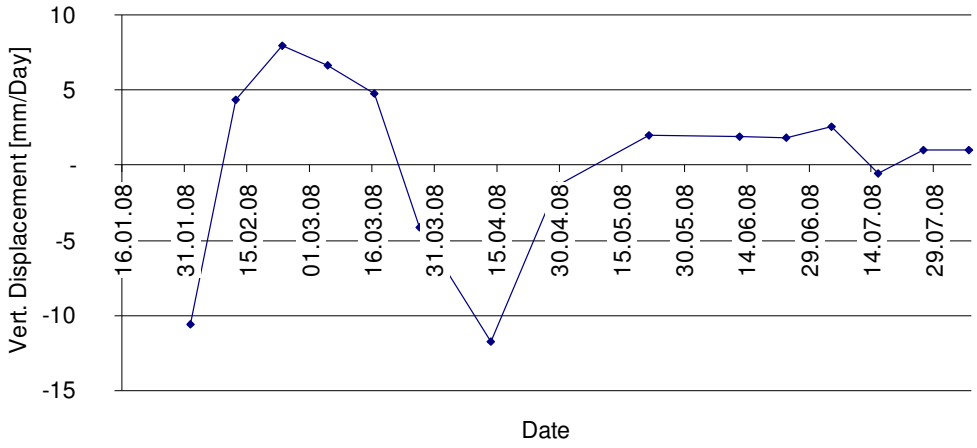


Figure 9: Evolution of displacements on one specific point of interest (indicated by black cross in Figure 8) using selected interferograms with temporal baselines of 11 days

5.3 Comparison with DGPS data

For a large scale comparison of TerraSAR-X and GPS results, the 1. GPS campaign (23/01/2008 – 05/02/2008) was set as reference epoch for GPS analysis. The time period of the first GPS campaign is almost identical to the time period related to the first TerraSAR-X interferogram used as reference for integrated DInSAR results. The measured vertical movements of GPS points during the following campaigns were compared to the integrated results of TerraSAR-X. Figure 10 shows the differences of vertical movements of the 2. GPS campaign and the corresponding integrated DInSAR result of 24/04/2008. The points are categorized into classes with respect to the difference between DInSAR and GPS analyzes. It can be seen that the maximum difference of vertical movements derived from GPS and DInSAR is below 2 cm. The majority of the points show differences clearly below 1 cm.

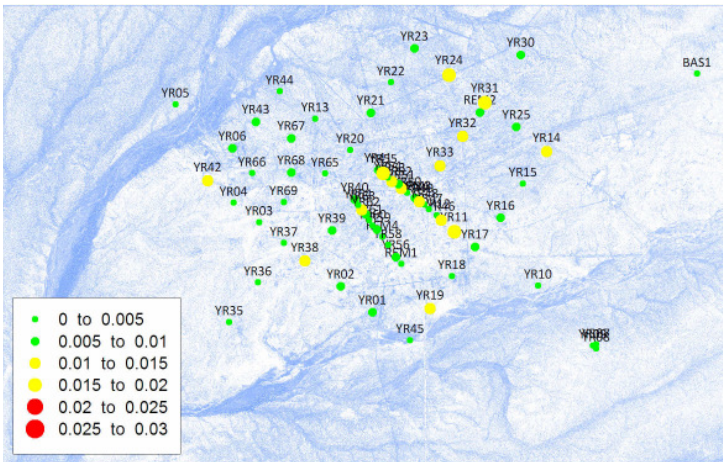


Figure 10: Differences (in [m]) of vertical surface displacement between TerraSAR-X integrated deformation map (20080424) and results of 2. GPS campaign (20080410 – 20080423)

The permanently observed GPS points REM 1 to REM 4 were compared to TerraSAR-X DInSAR derived vertical movements. Figure 11 shows the corresponding illustration for the time series of vertical displacements at GPS point REM 1 in comparison to TerraSAR-X derived results. Except for deviations due to atmospheric phase a good correlation between GPS and TerraSAR-X results can be stated.

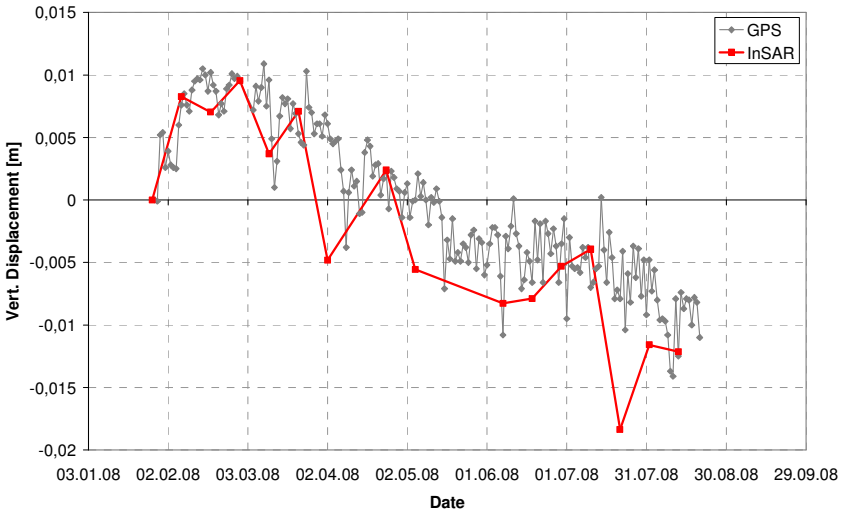


Figure 11: Vertical movement with time of GPS point "REM1" and movement of corresponding TerraSAR-X deformation map

6 Conclusion

The study results demonstrate that TerraSAR-X interferometry is suited for determination of large-scale relatively uniform as well as small-scale highly dynamic surface displacements. Some of the results could be validated with GPS measurements. The comparison of TerraSAR-X results and GPS measurements showed a good correlation for dynamic movements as well as for the slower, relatively uniform displacements.

In the case of large-scale temporally relatively uniform subsidence at relatively low rates displacement maps generated from single interferograms reveal distortions by atmospheric path delay effects. Nevertheless, by integrating subsequent short interval results, the dominating surface movement could be identified and quantified. The good temporal sampling achieved with the 11 day repeat cycle of TerraSAR-X permits a better suppression of atmospheric errors, e.g. by temporal filtering. In the context of oil field monitoring this clearly indicates a good potential of high resolution interferometry using TerraSAR-X for precise monitoring of "conventional" oil production sites with large-scale temporally relatively uniform subsidence.

TerraSAR-X interferometry was also efficiently used for the monitoring of stronger and more dynamic movements, thanks to its high spatial and temporal resolution capability. This is potentially of interest for the monitoring of more dynamic surface movements as occurring in the case of oil production supported by man-made injection and other production measures (e.g. Enhanced Oil Recovery - EOR), especially in the case of varying injection and production rates.

Small-scale surface displacement responses for example related to a spatially dense grid of injection/production wells and/or well casings potentially leaking in shallow subsurface structures can also be resolved by radarinterferometric processing of high resolution SAR data (e.g. TerraSAR-X).

Acknowledgements

TerraSAR-X data used for this study were provided by Infoterra Germany. Processing for the study was conducted by Gamma Remote Sensing AG (Switzerland), Infoterra (Germany) and DMT GmbH & Co. KG (Germany). Petroleum Development of Oman (PDO), contributed ancillary data and interpretation of results.